Published in final edited form as:

Mol Microbiol. 2016 April ; 100(1): 1–14. doi:10.1111/mmi.13284.

Dead-end intermediates in the enterobacterial common antigen pathway induce morphological defects in *Escherichia coli* by competing for undecaprenyl phosphate

Matthew A. Jorgenson, **Suresh Kannan**, **Mary E. Laubacher**[1], and **Kevin D. Young**[1]

Department of Microbiology and Immunology, University of Arkansas for Medical Sciences, Little Rock, AR 72205, USA

Summary

Bacterial morphology is determined primarily by the architecture of the peptidoglycan (PG) cell wall, a mesh-like layer that encases the cell. To identify novel mechanisms that create or maintain cell shape in *Escherichia coli*, we used flow cytometry to screen a transposon insertion library and identified a *wecE* mutant that altered cell shape, causing cells to filament and swell. WecE is a sugar aminotransferase involved in the biosynthesis of enterobacterial common antigen (ECA), a non-essential outer membrane glycolipid of the *Enterobacteriaceae*. Loss of *wecE* interrupts biosynthesis of ECA and causes the accumulation of the undecaprenyl pyrophosphate linked intermediate ECA-lipid II. The *wecE* shape defects were reversed by: (i) preventing initiation of ECA biosynthesis, (ii) increasing the synthesis of the lipid carrier undecaprenyl phosphate (Und-P), (iii) diverting Und-P to PG synthesis, or (iv) promoting Und-P recycling. The results argue that the buildup of ECA-lipid II sequesters part of the pool of Und-P, which, in turn, adversely affects PG synthesis. The data strongly suggests there is competition for a common pool of Und-P, whose proper distribution to alternate metabolic pathways is required to maintain normal cell shape in *E. coli*.

Keywords

undecaprenyl phosphate; enterobacterial common antigen; peptidoglycan; bacterial morphology; sequestration

Introduction

Bacteria display a wide diversity of shapes and sizes, and these morphologies remain remarkably constant from one generation to the next (reviewed in Young, 2006). With a few notable exceptions (e.g. *Mycoplasma*), bacterial morphology is determined primarily by the architecture of the peptidoglycan (PG) wall, a mesh-like layer that encases the cell and protects it against turgor force (reviewed in Vollmer *et al*., 2008a). PG consists of glycan strands composed of the repeating disaccharide, *N*-acetylglucosamine (GlcNAc) and *N*-acetylmuramic acid (MurNAc), and these glycan strands are cross-linked to one another by

[1]Corresponding author: kdyoung@uams.edu, Phone: 501-526-6802, Fax: 501-686-5359.
[1]Current address: Monsanto Company, 800 North Lindbergh Boulevard, St. Louis, MO 63167

short peptides extending from the MurNAc residue. In the Gram-negative bacterium *Escherichia coli*, PG biosynthesis begins in the cytoplasm and results in the formation of a GlcNAc-MurNAc-pentapeptide linked to the carrier lipid undecaprenyl phosphate (Und-P) to form lipid II, hereafter referred to as PG-lipid II (reviewed in Bouhss *et al.*, 2008, Typas *et al.*, 2012). PG-lipid II is translocated to the periplasmic space by a flippase (Mohammadi *et al.*, 2011, Sham *et al.*, 2014), and the newly flipped GlcNAc-MurNAc-pentapeptide moiety is inserted into the growing PG chain. PG synthesis is driven by a complex of proteins whose activities are directed by the actin homolog MreB during cell elongation and by the tubulin homolog FtsZ during cell division (reviewed in den Blaauwen *et al.*, 2008, Young, 2010, Egan & Vollmer, 2013). In addition, PG hydrolases facilitate growth and separation of daughter cells by cleaving selected bonds within the PG layer (reviewed in Vollmer *et al.*, 2008b, van Heijenoort, 2011). Mutations affecting PG synthesis or degradation can cause defects in cell wall assembly, leading to shape abnormalities that include filamentation, branching, chaining, rounding, spiraling, and swelling (de Pedro *et al.*, 2003, Heidrich *et al.*, 2001, Iwaya *et al.*, 1978, Varma & Young, 2004).

Much of our understanding of how bacteria establish and maintain their shapes is derived from mutations that directly affect PG synthesis and degradation. However, new and unexpected connections between metabolism and morphogenesis are expanding our view of how cell shape is regulated (reviewed in Vadia & Levin, 2015). For example, in *Bacillus subtilis*, the accumulation of UDP-glucose facilitates an interaction between the glucosyltransferase UgtP and FtsZ (Weart *et al.*, 2007). When grown in rich medium, the UgtP-FtsZ interaction disrupts assembly of the cell division apparatus, which delays cytokinesis and causes cells to grow longer before they divide. In *E. coli*, the glucosyltransferase OpgH mediates an analogous reaction (Hill *et al.*, 2013). In *Caulobacter crescentus*, the oxidoreductase-like KidO and the NAD-dependent glutamate dehydrogenase GdhZ promote FtsZ-ring (Z-ring) disassembly. The levels of KidO and GdhZ oscillate with the cell cycle to stimulate cytokinesis and prevent premature assembly of the Z-ring (Radhakrishnan *et al.*, 2010, Beaufay *et al.*, 2015). Finally, *E. coli* mutants lacking the fatty acid synthase FabH cannot change size in response to nutrient availability, thus implicating fatty acid biosynthesis in cell size regulation (Yao *et al.*, 2012).

These associations between cell shape and metabolism suggest that there are alternate ways by which bacteria can control their dimensions. Therefore, to identify new morphological mechanisms and regulators, we developed a flow cytometry-based screen to look for novel shape mutants in *E. coli*. Flow cytometry can distinguish minor shape alterations among bacterial populations and can be used to select for mutants that suppress highly aberrant morphologies, or that are enriched for shape defects (Meberg *et al.*, 2004, Laubacher *et al.*, 2013, Burke *et al.*, 2013, Sycuro *et al.*, 2013). This ability to analyze a heterogeneous population and capture cells with altered shapes makes flow cytometry a powerful tool for morphological studies.

Here, we screened a transposon insertion library by flow cytometry and found that a mutation in *wecE* created morphological abnormalities. WecE is involved in the biosynthesis of enterobacterial common antigen (ECA), a non-essential glycolipid found in the outer membrane of *Enterobacteriaceae*. A *wecE* mutant accumulates the ECA intermediate lipid II

(ECA-lipid II), which triggers several cell envelope stress responses and confers sensitivity to bile salts (Danese *et al.*, 1998). However, the mechanism by which ECA-lipid II exerts these effects is unknown. The present results suggest that the accumulation of ECA-lipid II (and more broadly other Und-P-utilizing glycan intermediates) sequesters part of the pool of free Und-P, which apparently restricts or alters PG synthesis. We conclude that alternate metabolic pathways compete for a common pool of Und-P, whose balanced distribution is required to maintain proper cell shape in *E. coli*.

Results

A genetic shape screen identifies a wecE mutant

We began to screen for novel shape and division mutants in *E. coli* by using a cell sorting assay previously employed to enrich for spontaneous shape suppressor mutants (Laubacher *et al.*, 2013). Wild type *E. coli* CS109 was mutagenized with EZTnKan-2 (Epicentre) to give a preliminary library of approximately 5,000 independent insertion mutants, which were pooled, grown in LB medium at 37°C and analyzed by flow cytometry. The shape distribution of the mutant population was nearly identical to CS109 (Fig. 1A and 1B). Given this, we defined a selection gate to sort aberrantly shaped cells from the mutant population. Burke *et al.* (Burke *et al.*, 2013) demonstrated that longer cells exhibit an increase in side scatter width (SSC-W), a measure of the time it takes a particle to pass through the fixed alignment laser in a flow cytometer. To confirm this observation, we filamented CS109 cells with aztreonam, which inhibits PG synthesis at the septum (Fig. 1C) (Georgopapadakou *et al.*, 1982). As expected, these elongated cells exhibited an increase in SSC-W and in side scatter height (SSC-H) (Fig. 1D).

We created a sorting gate (Fig. 1D, dotted rectangle) that encompassed ~80% of the aztreonam-treated cells, and collected the mutant population from within this gate (Fig. 1B, solid rectangle). These cells represented those that were either longer or larger than normal unit-sized wild type cells. Approximately 600 cells were collected from this gate and grown in LB medium at 37°C. Of these, 50% grew after overnight incubation. Remarkably, 99% of cells looked normal when reanalyzed by flow cytometry (not shown). This high false positive rate was most likely caused by transient filamentation of cells in the population, a phenomenon that is not understood (Burke *et al.*, 2013). A similar morphological instability occurs in the bacterium *Helicobacter pylori*, suggesting that transient shape alterations may be a general phenomenon (Sycuro *et al.*, 2013). Nevertheless, from 300 candidates we isolated three shape mutants, and we mapped the insertion points of each transposon by arbitrary PCR (Bernhardt & de Boer, 2004). One mutant produced a dramatic change in the shape distribution of its population (Fig. 1E and 1F), and the Tn insertion point in this strain was mapped to *tatC*. TatC is an essential subunit of the twin-arginine translocation system (TatABC) (reviewed in Palmer & Berks, 2012) that exports folded proteins to the periplasmic space, including the PG cell wall amidases AmiA and AmiC (Bernhardt & de Boer, 2003, Ize *et al.*, 2003). As expected, the insertion in *tatC* prevented AmiA and AmiC from processing PG during growth and division, causing the cells to grow as unseparated cells (Fig. 1E) (Bernhardt & de Boer, 2003, Ize *et al.*, 2003). Thus, isolation of this mutant served as a positive proof-of-principle for the cell sorting approach described here. A second

morphology-altering mutation mapped to a gene of unknown function, *yfiH*, whose characterization will be reported elsewhere (Jorgenson *et al.*, unpublished).

The third shape mutant contained an insertion that mapped to codon 163 of the *wecE* gene, which encodes a TDP-4-keto-6-deoxy-D-glucose aminotransferase that is required for elongating lipid III during the synthesis of ECA (Fig. 2A) (Meier-Dieter *et al.*, 1990, Hwang *et al.*, 2004). The distribution of the forward scatter area (FSC-A) of the *wecE*::Tn mutant population was shifted to the right (Fig. 1H), suggesting that the cells were enlarged, and microscopy confirmed that mutant cells were longer and wider than wild type (Fig. 1G). To confirm that the shape defects were caused by inactivation of *wecE* alone, we deleted *wecE* (Δ*wecE*) by lambda Red recombination (Datsenko & Wanner, 2000). This Δ*wecE* mutant exhibited the same phenotypes as the *wecE*::Tn mutant (not shown). Close inspection of the Δ*wecE* mutant grown in LB broth revealed that cells grew longer at elevated temperature (compare 25°C vs 37°C) and became noticeably swollen (25% wider than wild type) at 37°C (Table 1). Moreover, while the growth rate of the Δ*wecE* mutant was similar to the parent strain when grown at 25°C, 30°C and 37°C in LB broth, the mutant underwent a limited lysis shortly after being shifted to 42°C before resuming growth at rate similar to that of the wild type (Fig. S1). All morphological and growth defects were rescued by expressing *wecE* from a plasmid (Fig. 3A and 3B, and not shown).

wecE mutants prevent the formation of ECA-lipid III and therefore accumulate the intermediate ECA-lipid II (Fig. 2A) (Danese *et al.*, 1998). For unknown reasons, accumulating ECA-lipid II disrupts outer membrane integrity and produces sensitivity to sodium dodecyl sulfate and bile salts (Rick *et al.*, 1988, Danese *et al.*, 1998, Ramos-Morales *et al.*, 2003). Predictably, the growth of our Δ*wecE* mutant was inhibited on LB containing 1% deoxycholate (Fig. 4A), confirming that the outer membrane was defective.

ECA pathway mutants also trigger the Rcs stress response and inhibit motility (Castelli *et al.*, 2008, Castelli & Vescovi, 2011). As expected, motility was repressed in our Δ*wecE* mutant, and this defect was suppressed by deleting the Rcs regulator *rcsB* (Fig. S2). The Cpx stress response is also stimulated in *wecE* mutants and negatively regulates motility (Danese *et al.*, 1998, Evans *et al.*, 2013). To determine the contribution of the Cpx stress response on motility in the Δ*wecE* mutant, we deleted the Cpx response regulator, c*pxR*, from the Δ*wecE* mutant, but this had little effect (Fig. S2). Moreover, the migration of a Δ*wecE* Δ*rcsB* Δ*cpxR* mutant was indistinguishable from that of the Δ*wecE* Δ*rcsB* mutant (Fig. S2). These results indicate that the Cpx stress response does not significantly alter motility in Δ*wecE* mutants. Collectively, these data indicate that *wecE* is required to maintain normal cell shape and envelope integrity in *E. coli*.

ECA is not required to maintain proper cell shape

The morphological defects observed in Δ*wecE* cells suggested two possibilities: either ECA was required to maintain proper cell shape, or else shape defects were caused by the accumulation of ECA-lipid II. To distinguish between these alternatives, we first deleted *wecA*, whose gene product initiates ECA biosynthesis by transferring *N*-acetylglucosamine-1-phosphate (GlcNAc-1-P) onto the essential lipid carrier undecaprenyl phosphate (Und-P) to make Und-PP-GlcNAc (ECA-lipid I) (Fig. 2A). If ECA was required

to maintain normal cell shape, then a Δ*wecA* mutant should exhibit the same phenotype as the Δ*wecE* mutant. However, Δ*wecA* cells looked normal (Fig. 2B), although the forward scattered light of the Δ*wecA* mutant population shifted slightly to the right compared to the wild type (Fig. 2C). Since neither Δ*wecA* nor Δ*wecE* cells synthesize ECA (Fig. 2A), but the Δ*wecA* cells retained their normal rod shapes, the results demonstrated that ECA itself was not required to maintain wild type morphology. This suggested that accumulation of ECA-lipid II was responsible for the shape defects in Δ*wecE* cells. If true, then deleting *wecA* should reverse the shape defects caused by the *wecE* mutation, because ECA-lipid II would no longer be synthesized. Consistent with this prediction, the cells of a Δ*wecE* Δ*wecA* double mutant were of normal shape (Fig. 2B and 2C), indicating that the accumulation of ECA-lipid II was in some way responsible for the shape defects.

ECA-lipid II accumulation probably sequesters Und-P

The shape defects in Δ*wecE* cells suggested that ECA-lipid II might exert an indirect effect on PG synthesis by sequestering undecaprenyl phosphate (Und-P), the lipid carrier that transfers both PG and ECA intermediates across the inner membrane (reviewed in Bouhss *et al.*, 2008). This scenario parallels what has been observed in Gram positive bacteria. Specifically, depleting an essential late acting enzyme from the wall teichoic acid (WTA) biosynthesis pathway causes the accumulation of undecaprenyl pyrophosphate (Und-PP)-linked WTA intermediates and reduces the incorporation of new PG (D'Elia *et al.*, 2009). Interestingly, the addition of exogenous Und-P suppresses these effects (Farha *et al.*, 2015). Thus, if a limited amount of free Und-P inhibited PG synthesis in the Δ*wecE* mutant, then synthesizing more Und-P should reverse the shape defects by supplying enough substrate to satisfy the needs of both pathways. We increased the pool of Und-P by overexpressing the Und-PP synthase, encoded by *uppS* (also known as *ispU*), which is involved in the *de novo* synthesis of Und-P. UppS overproduction in the Δ*wecE* mutant fully reversed the shape defects, as visualized by microscopy and flow cytometry (Fig. 3A and 3B), suggesting that accumulation of ECA-lipid II had reduced the pool of freely available Und-P, which thereby restricted or altered PG synthesis via competitive inhibition.

Overexpressing *bacA*, which converts Und-PP to Und-P, is also thought to increase the available pool of Und-P (Cain *et al.*, 1993). However, overexpressing *bacA* did not reverse the shape defects of Δ*wecE* cells (Fig. 3A and 3B), and deleting *bacA* did not exacerbate the shape defect (Fig. S4C and S4D). It may be that BacA does not alter the overall pool size of Und-P in this context.

An alternate method for reversing the effects of substrate competition is to increase the competitive advantage of one pathway over another. MurA is a PG transferase that competes with WecA for the common starting substrate in both pathways, UDP-GlcNAc (Marquardt *et al.*, 1992). Thus, redirecting UDP-GlcNAc into the PG pathway by overexpressing *murA* might reverse the shape defects of Δ*wecE* cells by increasing the flux of Und-P toward PG synthesis and restricting its availability for the ECA pathway. In fact, overexpressing *murA* suppressed the shape defects of Δ*wecE* cells, consistent with the competition hypothesis (Fig. 3A and 3B).

The ECA pathway also competes for substrates with the O-antigen pathway. However, most *E. coli* K-12 strains (including CS109) do not produce O-antigen because of an IS5 insertion into *wbbL* (Liu & Reeves, 1994). ECA-lipid I is the substrate for both WbbL, a rhamnose transferase in the O-antigen pathway, and for WecG in the ECA pathway (Fig. 2A). Therefore, redirecting ECA-lipid I might also increase the pool of free Und-P by promoting Und-P recycling through the O-antigen pathway and thus preventing this substrate from reaching the dead-end ECA pathway in Δ*wecE* cells. Indeed, multicopy expression of *wbbL* reversed the shape defects of Δ*wecE* cells (Fig. 3A and 3B), consistent with the idea that ECA-lipid II accumulation adversely affects the amount of Und-P available for PG synthesis. Reconstitution of the O-antigen by *wbbL* overexpression was verified by detection with Concanavalin A (not shown) (Ghosh & Young, 2005). Overexpression of the above genes had no discernable effect on cell shape (Fig. S3A and S3B).

Overall, the results strongly suggest that accumulation of ECA-lipid II in a Δ*wecE* mutant indirectly affects PG synthesis by sequestering part of the pool of freely available Und-P.

Correcting the shape defects of ΔwecE cells stabilizes the outer membrane

Defects in septal PG synthesis and cell division disrupt the barrier function of the outer membrane, conferring sensitivity to bile salts (Heidrich *et al.*, 2002, Arends *et al.*, 2010). If the accumulation of ECA-lipid II affected PG synthesis by the sequestration model, then correcting the shape defects by promoting the flux of Und-PP-linked intermediates into the PG pathway might also reverse deoxycholate sensitivity of the Δ*wecE* mutant. Indeed, overexpressing *uppS* and *murA*, but not *bacA*, restored deoxycholate resistance to the Δ*wecE* mutant (Fig. 4B). Overexpressing *wbbL* (Fig. 4B) or deleting *wecA* (Fig. 4A) only partially reversed the Δ*wecE* membrane defect, suggesting that membrane integrity is sensitive to minor alterations in cell shape, whose presence may be below our limit of detection. Alternately, membrane defects may be independent of cell shape under certain conditions. In either case, accumulation of ECA-lipid II in the Δ*wecE* mutant seems to confer bile salt sensitivity by restricting or altering PG synthesis.

Correcting the shape defect of ΔwecE cells represses the Rcs response

When ECA-lipid II accumulates, the Rcs stress system is induced by an unknown mechanism (Castelli & Vescovi, 2011). Interestingly, minor alterations in PG structure also induce the Rcs stress response and inhibit motility (Laubacher & Ades, 2008, Evans *et al.*, 2013). If deleting *wecE* stimulated the Rcs pathway, then increasing the amount of Und-P available for PG synthesis should reverse the motility defect. Consistent with this prediction, overexpressing *uppS*, *murA*, or *wbbL*, but not *bacA*, reversed the motility defect of the Δ*wecE* mutant (Fig. 5B). Deleting *wecA* also partially rescued motility (Fig. S2). Overexpressing these genes had little effect on WT motility (Fig. 5A). Thus, accumulation of ECA-lipid II probably triggers the Rcs stress response by limiting the amount of substrate available for PG synthesis.

Other ECA mutants exhibit shape defects

If Und-P was sequestered by the accumulation of ECA-lipid II, then removing other proteins in the ECA pathway should have similar effects, as long as these mutants would also

accumulate Und-PP-linked intermediates. As expected, a Δ*wzxE* (ECA flippase) mutant (Fig. 2A) exhibited morphological abnormalities similar to those of the Δ*wecE* mutant (Fig. 6A and 6B). Mutants lacking *wecB*, *wecF*, or *wecG* (Fig. 2A) also exhibited shape defects, though these were less severe than those of the Δ*wecE* mutant (Fig. 6A and 6B). A Δ*wecA* mutation (Fig. 2A) had little effect on cell shape (Fig. 2B and 2C), as did a Δ*rffH* mutation (Fig. 6A and 6B). However, lesions in *rffH* do not inhibit ECA synthesis because, in *E. coli*, RmlA substitutes for the loss of RffH (Fig. 2A) (Marolda & Valvano, 1995, Danese *et al.*, 1998). The results support the interpretation that cell shape defects are caused by indirect effects associated with the accumulation of ECA intermediates.

The Rcs response does not exacerbate morphological defects in the ΔwecE mutant

The Rcs phosphorelay response initiates the synthesis of the extracellular polysaccharide colanic acid, whose biosynthesis also requires Und-P (reviewed in Majdalani & Gottesman, 2005, Whitfield, 2006). Synthesizing this compound would also increase the demand on the available pool of Und-P and might therefore exacerbate the morphological defects of Δ*wecE* cells. However, deleting *rcsB* did not reverse the shape defects of Δ*wecE* cells (Fig. S4C and S4D). Moreover, deleting *wcaJ*, whose gene product transfers colanic acid precursors onto Und-P (Patel *et al.*, 2012), did not alleviate shape defects (Fig. S4C and S4D). Deleting *rcsB* or *wcaJ* had no effect on shape (Fig. S4A and S4B). Thus, the shape defects of Δ*wecE* cells were independent of the Rcs response.

Overexpressing elyC or mrcB does not reverse the morphological defects of ΔwecE cells

Paradis-Bleau *et al.* reasoned that a newly-discovered protein encoded by the *elyC* gene might be involved in moderating a competition between the PG and ECA biosynthesis pathways, probably at the level of Und-P metabolism (Paradis-Bleau *et al.*, 2014). An *elyC* mutant exhibits growth and membrane defects that are reminiscent of those in a Δ*wecE* mutant, defects that are reversed by overexpressing *uppS*, *murA*, or *mrcB*, and by mutations that block ECA production (Paradis-Bleau *et al.*, 2014). The parallels between the *elyC* and *wecE* phenotypes suggested that overexpressing *elyC* or *mrcB* might also reverse the shape defects of a Δ*wecE* mutant, perhaps by shifting Und-P utilization towards PG synthesis. However, overexpressing *elyC* or *mrcB* did not restore normal shape to the Δ*wecE* mutant (Fig. S5). While this was somewhat surprising, the function of ElyC is more important at lower temperatures, whereas the Δ*wecE* phenotypes are more prominent at higher temperatures. Thus, *elyC* and *wecE* appear to affect the balance of Und-P by different mechanisms.

Discussion

Bacteria produce their specific shapes by regulating PG synthesis as the cells elongate via an MreB-dependent mechanism (Billings *et al.*, 2014, Tropini *et al.*, 2014, Si *et al.*, 2015), as they divide via an FtsZ-dependent mechanism (Varma & Young, 2004, Varma *et al.*, 2007, Varma & Young, 2009, Potluri *et al.*, 2012), or by mechanisms that involve accessory PG hydrolases (Heidrich *et al.*, 2002, Priyadarshini *et al.*, 2007, Singh *et al.*, 2012). A more recent discovery is that intermediates of glucose metabolism inhibit FtsZ-driven cell division, thereby explaining the decades-old observation that fast growing cells are longer

and larger (Weart *et al.*, 2007, Hill *et al.*, 2013). Here, we show that the morphology of *E. coli* is also sensitive to alterations in the distribution of shared lipid-linked precursors among pathways that synthesize PG, ECA, and O-antigen. This conclusion was triggered by finding that cells lacking an ECA pathway enzyme, the aminotransferase WecE, exhibited abnormal cell shapes. *wecE* mutants accumulate the Und-PP-linked compound, ECA-lipid II (Danese *et al.*, 1998), a dead-end intermediate that might therefore sequester part of the pool of free Und-P, which is required for PG synthesis. The results imply that the PG and ECA biosynthetic pathways, as well as those that synthesize other glycan polymers, compete for a common pool of Und-P (Fig. 7) (Paradis-Bleau *et al.*, 2014). In short, bacterial morphology is determined not only by the synthases and hydrolases that create and modify the cell wall, but also by the physiological processes that distribute shared precursors among these related pathways.

Explaining the toxicity of Und-PP-linked polysaccharide intermediates

The deleterious effects triggered by the accumulation of various Und-PP-linked metabolic intermediates have been known for some time (Yuasa *et al.*, 1969, Rick *et al.*, 1988, Danese *et al.*, 1998, Rick *et al.*, 2003, Marolda *et al.*, 2006, Tatar *et al.*, 2007, Castelli & Vescovi, 2011), but the mechanism of this toxicity has remained elusive. In theory, there are three possible explanations. First, the end product (in this case ECA) might be required for creating the wild type shape of *E. coli*. However, cells lacking *wecA* grew as normally shaped rods, even though this mutation prevents the production of ECA (Meier-Dieter *et al.*, 1990). Also, deleting *wecA* reversed the morphological defects of the *wecE* mutant. These results argue that the lack of ECA does not produce the negative physiological phenotypes. The second alternative is that the compound that accumulates (in this case ECA-lipid II) is toxic in and of itself, perhaps because it cannot be translocated to the periplasm and thereby poisons some essential reaction. This is the simplest and most direct interpretation (Danese *et al.*, 1998, Rick *et al.*, 2003, Marolda *et al.*, 2006). However, the toxic effects of a *wecE* mutation are suppressed by increasing the precursor pool of Und-P. Since the amount of any putative intermediate should not change in this circumstance (and might even increase), it is unlikely that the accumulated compound behaves like a classic toxin, in the sense of inhibiting some other reaction directly and specifically.

The third and most likely possibility is that trapping more and more material in a dead-end intermediate is deleterious because it sequesters a precursor that is required for another purpose. In this case, accumulation of ECA-lipid II would reduce the pool of free Und-P available for other pathways, namely those that synthesize PG, O-antigen, or colanic acid (Fig. 7). Strong support for this interpretation is provided by the fact that increasing the total pool of Und-P reverses the phenotypic effects of a *wecE* mutation, as does redirecting more of the limited pool of free Und-P into the PG synthetic pathway. In addition, cells containing a temperature sensitive allele of *uppS* have decreased levels of Und-P and exhibit shape defects that look remarkably similar to those of a *wecE* mutant (Kato *et al.*, 1999), further supporting the idea that reducing the availability of Und-P is detrimental to cell wall synthesis. In a possible counter-example, Danese *et al.* found it unlikely that ECA-lipid II accumulation would affect PG synthesis by sequestering Und-P because its effects were not reversed by overexpressing the Und-PP phosphatase *bacA* (Danese *et al.*, 1998). However,

our results suggest that accumulation of ECA-lipid II would also reduce the amount of free Und-PP, meaning that increasing or decreasing BacA levels may have little or no effect on the availability of Und-P. Taking the evidence as a whole, we conclude that the accumulation of Und-PP-linked intermediates indirectly restricts PG synthesis by sequestering Und-P, thereby impeding cell growth and producing morphological and membrane defects in *E. coli*.

Given the central role of Und-P in the biosynthesis of various glycan polymers, it should come as little surprise that the sequestration hypothesis has been suggested to account for several phenotypes observed in a diverse set of organisms including: *E. coli* (Paradis-Bleau *et al.*, 2014), *Salmonella enterica* (Yuasa *et al.*, 1969, Liu *et al.*, 2015), *Shigella dysenteriae* (Klena & Schnaitman, 1993), *Pseudomonas aeruginosa* (Burrows & Lam, 1999), *Bacillus subtilis* (D'Elia *et al.*, 2009), and *Streptococcus pneumoniae* (Xayarath & Yother, 2007). Thus, the sequestration of Und-P into non-productive intermediate compounds may explain many previous results obtained across a fairly wide range of bacteria. For example, overproducing WecA in an *E. coli wzxB wzxE* mutant causes the cells to elongate and then lyse, presumably because they produce an elevated amount of ECA-lipid III that cannot be exported to the periplasm (Rick *et al.*, 2003, Marolda *et al.*, 2006). ECA-lipid III accumulation would be expected to sequester Und-P (see Fig. 2A), and excess WecA would force even more of the Und-P pool into this non-productive pathway at the expense of PG synthesis, thus leading to the morphological alterations and lysis. Growth and morphological defects are also observed in mutants that accumulate Und-PP-linked O-antigen intermediates. Such mutants are genetically unstable (Yuasa *et al.*, 1969) and cause significant growth defects (Klena & Schnaitman, 1993), which suggested to Tatar *et al.* that these unprocessed intermediates were toxic (Tatar *et al.*, 2007). However, given our current results, it seems just as likely that these dead-end intermediates sequestered part of the pool of Und-P, thereby affecting PG synthesis and producing the phenotypes. Finally, the accumulation of ECA intermediates disrupts the bacterial membrane, confers sensitivity to detergents and bile salts, and induces the Cpx and Rcs stress responses (Rick *et al.*, 1988, Danese *et al.*, 1998, Castelli & Vescovi, 2011), all of which can also be caused by inhibiting PG synthesis (Laubacher & Ades, 2008, Evans *et al.*, 2013). Thus, the simplest unitary explanation that explains the effects associated with the accumulation of different compounds in related pathways is that in each case part of the pool of Und-P becomes trapped in an unusable intermediate. The similar phenotypes in these disparate systems would therefore arise from the common, indirect mechanism of inhibiting or otherwise affecting PG synthesis.

The above precursor sequestration interpretation coincides exactly with the explanation for how similar growth and morphological effects are produced by mutations in interrelated cell wall pathways in Gram positive bacteria. For example, in *B. subtilis*, blocking the late stages of wall teichoic acid (WTA) biosynthesis leads to shape defects and lysis (Brandt & Karamata, 1987, Briehl *et al.*, 1989, Pooley *et al.*, 1991, Bhavsar *et al.*, 2001, D'Elia *et al.*, 2006a), as it also does in *Staphylococcus aureus* (D'Elia *et al.*, 2006b, Campbell *et al.*, 2012). Mutations that block capsule synthesis in *S. pneumoniae* produce similar results (Xayarath & Yother, 2007). However, removing the first enzyme in these pathways is not lethal and, in fact, reverses the lethality of mutations affecting later steps in the pathway

(D'Elia *et al.*, 2006a, D'Elia *et al.*, 2006b, Xayarath & Yother, 2007), results that exactly parallel the phenomenon we report here. These previous authors speculated that the lethality was caused either by a buildup of toxic intermediates or because these intermediates trapped so much Und-P that PG synthesis was impaired. This latter possibility is identical to the Und-P sequestration mechanism we find to be at work here. Indeed, while the current manuscript was in preparation and under review, Farha *et al.* distinguished between these two possibilities in *S. aureus* by showing that the effect of late stage WTA mutations were reversed by adding exogenous Und-P, strongly supporting the idea that toxic intermediate compounds were not at fault but that Und-P was being sequestered (Farha *et al.*, 2015). We propose that this same phenomenon occurs in *E. coli* by virtue of the fact that different cell envelope pathways compete for this universal lipid carrier (Fig. 7).

Implications and unanswered questions

The fact that multiple synthetic pathways compete for Und-P raises several questions. First, does *E. coli* maintain a common pool of Und-P that can be accessed by any needy pathway? Although this seems most likely, current data cannot rule out the possibility that each pathway is fed by a dedicated sub-pool, though these might be supplemented by drawing from a shared pool. Second, regardless of whether there is one pool or several, it is not clear how the cell prioritizes and distributes Und-P among the various pathways, whether this be during normal growth conditions or in response to antibiotics or other environmental cues. PG synthesis is an obvious priority, but scenarios may arise in which other polysaccharides are deemed more vital in the short run. Can the cell redirect Und-P in these situations? Third, is the total amount of Und-P modulated in response to changing demands, and if so, how? On the surface, it would seem that a simple feedback mechanism could adjust the pool of Und-P, but whether this occurs is not known. However, even if such a homeostatic mechanism exists, it must not be very robust since it is obvious that significant deviations in the availability of Und-P can be produced by somewhat minor alterations in the demands made by competing pathways.

The present results also address the nature of one possible signal that has been suggested to induce the Rcs envelope stress response in *E. coli* (Majdalani & Gottesman, 2005). Defects in ECA biosynthesis trigger this response (thereby inhibiting bacterial motility), which seems to imply that the absence of periplasmic ECA is one of the signals that can induce the Rcs cascade (Castelli & Vescovi, 2011). However, our current results throw such a conclusion into doubt, because the Δ*wecE* motility defect can be rescued even when mature ECA structures are absent. Thus, the lack of ECA does not, by itself, function as an Rcs system inducer.

As mentioned earlier, mutations that impact cell shape are explained most easily by how they affect MreB-directed cell wall elongation or FtsZ-mediated division. PG synthesis is central to each process, so that in a *wecE* mutant each pathway is probably constrained by having decreased access to PG-lipid II. That a Δ*wecE* mutation elicits a filamentation phenotype suggests that cell division is more sensitive than is elongation to alterations in the pool of Und-P. Interestingly, in *B. subtilis*, PG-lipid II appears to be required for MreB to associate with the membrane and to form protein filaments (Schirner *et al.*, 2015). The fact

that an *E. coli wecE* mutant elongates suggests that a similar relationship may exist between PG-lipid II and one or more cell division proteins.

Finally, competition for Und-P provokes the intriguing possibility that this was the selective pressure that removed the O-antigen from most strains of *E. coli* K12 via a single IS element insertional event (Liu & Reeves, 1994). Because this strain has been incubated for decades under extremely growth-friendly laboratory conditions, it is easy to imagine that a growth advantage would accrue to cells that had eliminated one or more of the competitor pathways, thereby increasing the pool of Und-P available for the more relevant synthesis of PG. Because O-antigen is not essential under these conditions, it is a prime candidate for removal. In fact, there are two mutations that inactivate O-antigen synthesis in different strains of *E. coli* K12 (Liu & Reeves, 1994), and both truncate the pathway at its first, WbbL-directed step (see Fig. 7). Thus, no Und-PP-linked O-antigen intermediates accumulate in either case. It may be that these specific mutations were selected precisely because mutating any other downstream member of the pathway would produce dead-end Und-PP-linked intermediates that would produce growth defects as bad (or worse) than those associated with similar ECA intermediates. Whether these mutations arose for this reason is purely speculative, of course, but it seems clear that there is no real pressure to restore the O-antigen to *E. coli* K12, and perhaps the competition for Und-P explains why.

Experimental procedures

Media

Unless otherwise noted, cells were grown in Luria-Bertani (LB) broth (Difco). Plates contained 1.5% agar. Ampicillin, kanamycin, and tetracycline were used at 100, 50, and10 μg ml^{-1}, respectively. Migration plates contained 1% tryptone, 0.25% NaCl, and 0.25% agar.

Strains and plasmids

All strains, plasmids, and primers are listed in Tables S1, S2, and S3, respectively. Strain and plasmid construction is detailed in the supporting information. All plasmids used for *in vivo* experiments are derivatives of pDSW204 (Weiss *et al.*, 1999). Oligonucleotide primers and synthetic genes were purchased from Eurofins Genomics (Huntsville, Alabama).

Screening a transposon insertion library for cell shape mutants

Wild type CS109 cells were mutagenized with EZ-Tn-Kan2 (Epicentre), as described previously (Bernhardt & de Boer, 2004). The mutagenesis yielded approximately 5,000 colonies, which were pooled and diluted to an OD_{600} = 0.1 in LB medium. The mutant library was allowed to grow for 2 hours at 37°C to an OD_{600} = 0.6–0.7, after which cells were prepared for flow cytometry, as described previously (Laubacher *et al.*, 2013). Individual cells from the insertion library were sorted as described in the legend to Figure 1. Cells were sorted using a FACSAria III sorter from BD Biosciences (UAMS Flow Cytometry Core Facility) into a 96-well plate whose wells contained 0.15 mL LB. Plates were incubated at 37°C overnight, after which glycerol was added to a final concentration of 15% and the plates were stored at −80°C. Cells were rescreened for shape defects by growing overnight cultures in LB medium containing kanamycin at 37°C. Overnight

cultures were diluted 1:100 in LB medium at 37°C, grown to OD_{600} = 0.5–0.6, and analyzed by flow cytometry. Mutants that displayed a shift in FSC-A to the right (indicating larger cells) were confirmed by microscopy. The insertion point of the transposon was mapped by arbitrary PCR, as described (Bernhardt & de Boer, 2004).

Morphological analysis of the Δ*wecE* mutant

Overnight cultures grown at 37°C in LB medium were diluted 1:2000 in fresh LB medium and grown to OD_{600} = 0.5–0.6. Cells were stained with the membrane dye FM4-64 (Invitrogen), and 4 μl were spotted onto 1% agarose pads and visualized by phase-contrast and fluorescence microscopy.

Rescue of Δ*wecE* shape defects

Cells harboring plasmids were grown at 37°C in LB medium containing ampicillin. Overnight cultures were diluted 1:2000 in LB medium containing 50 μg ml^{-1} ampicillin and 25 μM IPTG and grown to an OD_{600} = 0.5–0.6 at 37°C. Cells were fixed, then photographed by phase-contrast microscopy. Live cells were used for flow cytometry analysis.

Flow cytometry analysis

Live cells were prepared for flow cytometry as described (Laubacher *et al.*, 2013). Overnight cultures grown in LB medium at 37°C were diluted 1:2000 in the same medium and grown to an OD_{600} = 0.5–0.6. Cells from 1 ml of an exponentially-growing culture were pelleted by centrifugation, and the resulting pellet was resuspended in 1 ml of filtered phosphate-buffered saline (PBS) (137 mM NaCl, 3 mM KCl, 9 mM NaH_2PO_4, and 2 mM KH_2PO_4, pH 7.4). Cells were washed twice in PBS, after which the cells were diluted 1:10 in PBS (OD_{600} ~ 0.05). Typical experiments analyzed 100,000 events (cells) using the forward- and side-scatter detectors in a BD LSRFortessa at the UAMS Flow Cytometry Core Facility.

Bile salt sensitivity assays

Overnight cultures grown in LB medium at 37°C were normalized to an OD_{600} = 1.0 in the same medium, and 10-fold serial dilutions were plated onto LB or LB containing 1% deoxycholate. Plates were incubated overnight at 37°C and then photographed.

Migration assays

Cells from 1.5 μl of an overnight culture grown at 30°C in LB were spotted onto the surface of a migration plate (Evans *et al.*, 2013). Plates were incubated at 30°C for 18 hours and then photographed.

Microscopy, image analysis, and figure construction

Our microscope and camera have been described previously (Vega & Young, 2014). Cell lengths were measured with cellSens Dimensions software version 1.6 (Olympus). Images were processed to adjust brightness and contrast using ImageJ (microscopy assays) (Schneider *et al.*, 2012) or Adobe Photoshop (migration assays). All images were cropped and assembled in Adobe Illustrator.

Supplementary Material

Refer to Web version on PubMed Central for supplementary material.

Acknowledgments

We thank Andrea Harris of the UAMS Flow Cytometry Core Facility for help with flow cytometry and analysis, and Allen Gies of the UAMS DNA Sequencing Core Facility for help with DNA sequencing. We thank Chris Whitfield, Kerry Evans, Dev Ranjit, William MacCain, and Daniel Vega for helpful discussions. We are grateful to Sarah Vestal for technical assistance. Research reported in this publication was supported by the National Institutes of General Medical Sciences award number GM061019.

References

Arends SJ, Williams K, Scott RJ, Rolong S, Popham DL, Weiss DS. Discovery and characterization of three new *Escherichia coli* septal ring proteins that contain a SPOR domain: DamX, DedD, and RlpA. J Bacteriol. 2010; 192:242–255. [PubMed: 19880599]

Beaufay F, Coppine J, Mayard A, Laloux G, De Bolle X, Hallez R. A NAD-dependent glutamate dehydrogenase coordinates metabolism with cell division in *Caulobacter crescentus*. EMBO J. 2015; 34:1786–1800. [PubMed: 25953831]

Bernhardt TG, de Boer PA. The *Escherichia coli* amidase AmiC is a periplasmic septal ring component exported via the twin-arginine transport pathway. Mol Microbiol. 2003; 48:1171–1182. [PubMed: 12787347]

Bernhardt TG, de Boer PA. Screening for synthetic lethal mutants in *Escherichia coli* and identification of EnvC (YibP) as a periplasmic septal ring factor with murein hydrolase activity. Mol Microbiol. 2004; 52:1255–1269. [PubMed: 15165230]

Bhavsar AP, Beveridge TJ, Brown ED. Precise deletion of *tagD* and controlled depletion of its product, glycerol 3-phosphate cytidylyltransferase, leads to irregular morphology and lysis of *Bacillus subtilis* grown at physiological temperature. J Bacteriol. 2001; 183:6688–6693. [PubMed: 11673441]

Billings G, Ouzounov N, Ursell T, Desmarais SM, Shaevitz J, Gitai Z, Huang KC. *De novo* morphogenesis in L-forms via geometric control of cell growth. Mol Microbiol. 2014; 93:883–896. [PubMed: 24995493]

Bouhss A, Trunkfield AE, Bugg TD, Mengin-Lecreulx D. The biosynthesis of peptidoglycan lipid-linked intermediates. FEMS Microbiol Rev. 2008; 32:208–233. [PubMed: 18081839]

Brandt C, Karamata D. Thermosensitive *Bacillus-subtilis* mutants which lyse at the nonpermissive temperature. Journal of General Microbiology. 1987; 133:1159–1170. [PubMed: 3116169]

Briehl M, Pooley HM, Karamata D. Mutants of *Bacillus-subtilis* 168 thermosensitive for growth and wall teichoic-acid synthesis. Journal of General Microbiology. 1989; 135:1325–1334.

Burke C, Liu M, Britton W, Triccas JA, Thomas T, Smith AL, Allen S, Salomon R, Harry E. Harnessing single cell sorting to identify cell division genes and regulators in bacteria. PLoS One. 2013; 8:e60964. [PubMed: 23565292]

Burrows LL, Lam JS. Effect of *wzx* (*rfbX*) mutations on A-band and B-band lipopolysaccharide biosynthesis in *Pseudomonas aeruginosa* O5. J Bacteriol. 1999; 181:973–980. [PubMed: 9922263]

Cain BD, Norton PJ, Eubanks W, Nick HS, Allen CM. Amplification of the *bacA* gene confers bacitracin resistance to *Escherichia coli*. J Bacteriol. 1993; 175:3784–3789. [PubMed: 8389741]

Campbell J, Singh AK, Swoboda JG, Gilmore MS, Wilkinson BJ, Walker S. An antibiotic that inhibits a late step in wall teichoic acid biosynthesis induces the cell wall stress stimulon in *Staphylococcus aureus*. Antimicrobial Agents and Chemotherapy. 2012; 56:1810–1820. [PubMed: 22290958]

Castelli ME, Fedrigo GV, Clementin AL, Ielmini MV, Feldman MF, Garcia Vescovi E. Enterobacterial common antigen integrity is a checkpoint for flagellar biogenesis in *Serratia marcescens*. J Bacteriol. 2008; 190:213–220. [PubMed: 17981971]

Castelli ME, Vescovi EG. The Rcs signal transduction pathway is triggered by enterobacterial common antigen structure alterations in *Serratia marcescens*. J Bacteriol. 2011; 193:63–74. [PubMed: 20971912]

D'Elia MA, Millar KE, Beveridge TJ, Brown ED. Wall teichoic acid polymers are dispensable for cell viability in *Bacillus subtilis*. J Bacteriol. 2006a; 188:8313–8316. [PubMed: 17012386]

D'Elia MA, Millar KE, Bhavsar AP, Tomljenovic AM, Hutter B, Schaab C, Moreno-Hagelsieb G, Brown ED. Probing teichoic acid genetics with bioactive molecules reveals new interactions among diverse processes in bacterial cell wall biogenesis. Chem Biol. 2009; 16:548–556. [PubMed: 19477419]

D'Elia MA, Pereira MP, Chung YS, Zhao W, Chau A, Kenney TJ, Sulavik MC, Black TA, Brown ED. Lesions in teichoic acid biosynthesis in *Staphylococcus aureus* lead to a lethal gain of function in the otherwise dispensable pathway. J Bacteriol. 2006b; 188:4183–4189. [PubMed: 16740924]

Danese PN, Oliver GR, Barr K, Bowman GD, Rick PD, Silhavy TJ. Accumulation of the enterobacterial common antigen lipid II biosynthetic intermediate stimulates *degP* transcription in *Escherichia coli*. J Bacteriol. 1998; 180:5875–5884. [PubMed: 9811644]

Datsenko KA, Wanner BL. One-step inactivation of chromosomal genes in *Escherichia coli* K-12 using PCR products. Proc Natl Acad Sci USA. 2000; 97:6640–6645. [PubMed: 10829079]

de Pedro MA, Young KD, Holtje JV, Schwarz H. Branching of *Escherichia coli* cells arises from multiple sites of inert peptidoglycan. J Bacteriol. 2003; 185:1147–1152. [PubMed: 12562782]

den Blaauwen T, de Pedro MA, Nguyen-Disteche M, Ayala JA. Morphogenesis of rod-shaped sacculi. FEMS Microbiol Rev. 2008; 32:321–344. [PubMed: 18291013]

Egan AJ, Vollmer W. The physiology of bacterial cell division. Ann NY Acad Sci. 2013; 1277:8–28. [PubMed: 23215820]

Evans KL, Kannan S, Li G, de Pedro MA, Young KD. Eliminating a set of four penicillin binding proteins triggers the Rcs phosphorelay and Cpx stress responses in *Escherichia coli*. J Bacteriol. 2013; 195:4415–4424. [PubMed: 23893115]

Farha MA, Czarny TL, Myers CL, Worrall LJ, French S, Conrady DG, Wang Y, Oldfield E, Strynadka NC, Brown ED. Antagonism screen for inhibitors of bacterial cell wall biogenesis uncovers an inhibitor of undecaprenyl diphosphate synthase. Proc Natl Acad Sci USA. 2015; 112:11048–11053. [PubMed: 26283394]

Georgopapadakou NH, Smith SA, Sykes RB. Mode of action of azthreonam. Antimicrob Agents Chemother. 1982; 21:950–956. [PubMed: 6180685]

Ghosh AS, Young KD. Helical disposition of proteins and lipopolysaccharide in the outer membrane of *Escherichia coli*. J Bacteriol. 2005; 187:1913–1922. [PubMed: 15743937]

Heidrich C, Templin MF, Ursinus A, Merdanovic M, Berger J, Schwarz H, de Pedro MA, Holtje JV. Involvement of *N*-acetylmuramyl-L-alanine amidases in cell separation and antibiotic-induced autolysis of *Escherichia coli*. Mol Microbiol. 2001; 41:167–178. [PubMed: 11454209]

Heidrich C, Ursinus A, Berger J, Schwarz H, Holtje JV. Effects of multiple deletions of murein hydrolases on viability, septum cleavage, and sensitivity to large toxic molecules in *Escherichia coli*. J Bacteriol. 2002; 184:6093–6099. [PubMed: 12399477]

Hill NS, Buske PJ, Shi Y, Levin PA. A moonlighting enzyme links *Escherichia coli* cell size with central metabolism. PLoS Genet. 2013; 9:e1003663. [PubMed: 23935518]

Hwang BY, Lee HJ, Yang YH, Joo HS, Kim BG. Characterization and investigation of substrate specificity of the sugar aminotransferase WecE from *E. coli* K12. Chem Biol. 2004; 11:915–925. [PubMed: 15271350]

Iwaya M, Goldman R, Tipper DJ, Feingold B, Strominger JL. Morphology of an *Escherichia coli* mutant with a temperature-dependent round cell shape. J Bacteriol. 1978; 136:1143–1158. [PubMed: 363690]

Ize B, Stanley NR, Buchanan G, Palmer T. Role of the *Escherichia coli* Tat pathway in outer membrane integrity. Mol Microbiol. 2003; 48:1183–1193. [PubMed: 12787348]

Kato J, Fujisaki S, Nakajima K, Nishimura Y, Sato M, Nakano A. The *Escherichia coli* homologue of yeast RER2, a key enzyme of dolichol synthesis, is essential for carrier lipid formation in bacterial cell wall synthesis. J Bacteriol. 1999; 181:2733–2738. [PubMed: 10217761]

Klena JD, Schnaitman CA. Function of the *rfb* gene cluster and the *rfe* gene in the synthesis of O antigen by *Shigella dysenteriae* 1. Mol Microbiol. 1993; 9:393–402. [PubMed: 7692219]

Laubacher ME, Ades SE. The Rcs phosphorelay is a cell envelope stress response activated by peptidoglycan stress and contributes to intrinsic antibiotic resistance. J Bacteriol. 2008; 190:2065–2074. [PubMed: 18192383]

Laubacher ME, Melquist AL, Chandramohan L, Young KD. Cell sorting enriches *Escherichia coli* mutants that rely on peptidoglycan endopeptidases to suppress highly aberrant morphologies. J Bacteriol. 2013; 195:855–866. [PubMed: 23243305]

Liu D, Reeves PR. *Escherichia coli* K12 regains its O antigen. Microbiology. 1994; 140(Pt 1):49–57. [PubMed: 7512872]

Liu MA, Stent TL, Hong Y, Reeves PR. Inefficient translocation of a truncated O unit by a *Salmonella* Wzx affects both O-antigen production and cell growth. FEMS Microbiol Lett. 2015:362.

Majdalani N, Gottesman S. The Rcs phosphorelay: a complex signal transduction system. Annu Rev Microbiol. 2005; 59:379–405. [PubMed: 16153174]

Marolda CL, Tatar LD, Alaimo C, Aebi M, Valvano MA. Interplay of the Wzx translocase and the corresponding polymerase and chain length regulator proteins in the translocation and periplasmic assembly of lipopolysaccharide o antigen. J Bacteriol. 2006; 188:5124–5135. [PubMed: 16816184]

Marolda CL, Valvano MA. Genetic analysis of the dTDP-rhamnose biosynthesis region of the *Escherichia coli* VW187 (O7:K1) *rfb* gene cluster: identification of functional homologs of *rfbB* and *rfbA* in the *rff* cluster and correct location of the *rffE* gene. J Bacteriol. 1995; 177:5539–5546. [PubMed: 7559340]

Marquardt JL, Siegele DA, Kolter R, Walsh CT. Cloning and sequencing of *Escherichia coli murZ* and purification of its product, a UDP-*N*-acetylglucosamine enolpyruvyl transferase. J Bacteriol. 1992; 174:5748–5752. [PubMed: 1512209]

Meberg BM, Paulson AL, Priyadarshini R, Young KD. Endopeptidase penicillin-binding proteins 4 and 7 play auxiliary roles in determining uniform morphology of *Escherichia coli*. J Bacteriol. 2004; 186:8326–8336. [PubMed: 15576782]

Meier-Dieter U, Starman R, Barr K, Mayer H, Rick PD. Biosynthesis of enterobacterial common antigen in *Escherichia coli*. Biochemical characterization of Tn10 insertion mutants defective in enterobacterial common antigen synthesis. J Biol Chem. 1990; 265:13490–13497. [PubMed: 2166030]

Mohammadi T, van Dam V, Sijbrandi R, Vernet T, Zapun A, Bouhss A, Diepeveen-de Bruin M, Nguyen-Disteche M, de Kruijff B, Breukink E. Identification of FtsW as a transporter of lipid-linked cell wall precursors across the membrane. EMBO J. 2011; 30:1425–1432. [PubMed: 21386816]

Palmer T, Berks BC. The twin-arginine translocation (Tat) protein export pathway. Nat Rev Microbiol. 2012; 10:483–496. [PubMed: 22683878]

Paradis-Bleau C, Kritikos G, Orlova K, Typas A, Bernhardt TG. A genome-wide screen for bacterial envelope biogenesis mutants identifies a novel factor involved in cell wall precursor metabolism. PLoS Genet. 2014; 10:e1004056. [PubMed: 24391520]

Patel KB, Toh E, Fernandez XB, Hanuszkiewicz A, Hardy GG, Brun YV, Bernards MA, Valvano MA. Functional characterization of UDP-glucose:undecaprenyl-phosphate glucose-1-phosphate transferases of *Escherichia coli* and *Caulobacter crescentus*. J Bacteriol. 2012; 194:2646–2657. [PubMed: 22408159]

Pooley HM, Abellan FX, Karamata D. A Conditional-Lethal Mutant of *Bacillus-Subtilis*-168 with a Thermosensitive Glycerol-3-Phosphate Cytidylyltransferase, an Enzyme Specific for the Synthesis of the Major Wall Teichoic-Acid. Journal of General Microbiology. 1991; 137:921–928. [PubMed: 1649892]

Potluri LP, de Pedro MA, Young KD. Escherichia coli low-molecular-weight penicillin-binding proteins help orient septal FtsZ, and their absence leads to asymmetric cell division and branching. Mol Microbiol. 2012; 84:203–224. [PubMed: 22390731]

Priyadarshini R, de Pedro MA, Young KD. Role of peptidoglycan amidases in the development and morphology of the division septum in *Escherichia coli*. J Bacteriol. 2007; 189:5334–5347. [PubMed: 17483214]

Radhakrishnan SK, Pritchard S, Viollier PH. Coupling prokaryotic cell fate and division control with a bifunctional and oscillating oxidoreductase homolog. Dev Cell. 2010; 18:90–101. [PubMed: 20152180]

Ramos-Morales F, Prieto AI, Beuzon CR, Holden DW, Casadesus J. Role for *Salmonella enterica* enterobacterial common antigen in bile resistance and virulence. J Bacteriol. 2003; 185:5328–5332. [PubMed: 12923112]

Rick PD, Barr K, Sankaran K, Kajimura J, Rush JS, Waechter CJ. Evidence that the *wzxE* gene of *Escherichia coli* K-12 encodes a protein involved in the transbilayer movement of a trisaccharide-lipid intermediate in the assembly of enterobacterial common antigen. J Biol Chem. 2003; 278:16534–16542. [PubMed: 12621029]

Rick PD, Wolski S, Barr K, Ward S, Ramsay-Sharer L. Accumulation of a lipid-linked intermediate involved in enterobacterial common antigen synthesis in *Salmonella typhimurium* mutants lacking dTDP-glucose pyrophosphorylase. J Bacteriol. 1988; 170:4008–4014. [PubMed: 2842298]

Schirner K, Eun YJ, Dion M, Luo Y, Helmann JD, Garner EC, Walker S. Lipid-linked cell wall precursors regulate membrane association of bacterial actin MreB. Nat Chem Biol. 2015; 11:38–45. [PubMed: 25402772]

Schneider CA, Rasband WS, Eliceiri KW. NIH Image to ImageJ: 25 years of image analysis. Nat Methods. 2012; 9:671–675. [PubMed: 22930834]

Sham LT, Butler EK, Lebar MD, Kahne D, Bernhardt TG, Ruiz N. Bacterial cell wall. MurJ is the flippase of lipid-linked precursors for peptidoglycan biogenesis. Science. 2014; 345:220–222. [PubMed: 25013077]

Si F, Li B, Margolin W, Sun SX. Bacterial growth and form under mechanical compression. Sci Rep. 2015; 5:11367. [PubMed: 26086542]

Singh SK, SaiSree L, Amrutha RN, Reddy M. Three redundant murein endopeptidases catalyse an essential cleavage step in peptidoglycan synthesis of *Escherichia coli* K12. Mol Microbiol. 2012; 86:1036–1051. [PubMed: 23062283]

Stevenson G, Neal B, Liu D, Hobbs M, Packer NH, Batley M, Redmond JW, Lindquist L, Reeves P. Structure of the O antigen of *Escherichia coli* K-12 and the sequence of its *rfb* gene cluster. J Bacteriol. 1994; 176:4144–4156. [PubMed: 7517391]

Sycuro LK, Rule CS, Petersen TW, Wyckoff TJ, Sessler T, Nagarkar DB, Khalid F, Pincus Z, Biboy J, Vollmer W, Salama NR. Flow cytometry-based enrichment for cell shape mutants identifies multiple genes that influence *Helicobacter pylori* morphology. Mol Microbiol. 2013; 90:869–883. [PubMed: 24112477]

Tatar LD, Marolda CL, Polischuk AN, van Leeuwen D, Valvano MA. An *Escherichia coli* undecaprenyl-pyrophosphate phosphatase implicated in undecaprenyl phosphate recycling. Microbiology. 2007; 153:2518–2529. [PubMed: 17660416]

Tropini C, Lee TK, Hsin J, Desmarais SM, Ursell T, Monds RD, Huang KC. Principles of bacterial cell-size determination revealed by cell-wall synthesis perturbations. Cell Rep. 2014; 9:1520–1527. [PubMed: 25456140]

Typas A, Banzhaf M, Gross CA, Vollmer W. From the regulation of peptidoglycan synthesis to bacterial growth and morphology. Nat Rev Microbiol. 2012; 10:123–136. [PubMed: 22203377]

Vadia S, Levin PA. Growth rate and cell size: a re-examination of the growth law. Curr Opin Microbiol. 2015; 24:96–103. [PubMed: 25662920]

van Heijenoort J. Peptidoglycan hydrolases of *Escherichia coli*. Microbiol Mol Biol Rev. 2011; 75:636–663. [PubMed: 22126997]

Varma A, de Pedro MA, Young KD. FtsZ directs a second mode of peptidoglycan synthesis in *Escherichia coli*. J Bacteriol. 2007; 189:5692–5704. [PubMed: 17513471]

Varma A, Young KD. FtsZ collaborates with penicillin binding proteins to generate bacterial cell shape in *Escherichia coli*. J Bacteriol. 2004; 186:6768–6774. [PubMed: 15466028]

Varma A, Young KD. In *Escherichia coli*, MreB and FtsZ direct the synthesis of lateral cell wall via independent pathways that require PBP 2. J Bacteriol. 2009; 191:3526–3533. [PubMed: 19346310]

Vega DE, Young KD. Accumulation of periplasmic enterobactin impairs the growth and morphology of *Escherichia coli tolC* mutants. Mol Microbiol. 2014; 91:508–521. [PubMed: 24330203]

Vollmer W, Blanot D, de Pedro MA. Peptidoglycan structure and architecture. FEMS Microbiol Rev. 2008a; 32:149–167. [PubMed: 18194336]

Vollmer W, Joris B, Charlier P, Foster S. Bacterial peptidoglycan (murein) hydrolases. FEMS Microbiol Rev. 2008b; 32:259–286. [PubMed: 18266855]

Weart RB, Lee AH, Chien AC, Haeusser DP, Hill NS, Levin PA. A metabolic sensor governing cell size in bacteria. Cell. 2007; 130:335–347. [PubMed: 17662947]

Weiss DS, Chen JC, Ghigo JM, Boyd D, Beckwith J. Localization of FtsI (PBP3) to the septal ring requires its membrane anchor, the Z ring, FtsA, FtsQ, and FtsL. J Bacteriol. 1999; 181:508–520. [PubMed: 9882665]

Whitfield C. Biosynthesis and assembly of capsular polysaccharides in *Escherichia coli*. Annu Rev Biochem. 2006; 75:39–68. [PubMed: 16756484]

Xayarath B, Yother J. Mutations blocking side chain assembly, polymerization, or transport of a Wzy-dependent *Streptococcus pneumoniae* capsule are lethal in the absence of suppressor mutations and can affect polymer transfer to the cell wall. J Bacteriol. 2007; 189:3369–3381. [PubMed: 17322316]

Yao Z, Davis RM, Kishony R, Kahne D, Ruiz N. Regulation of cell size in response to nutrient availability by fatty acid biosynthesis in *Escherichia coli*. Proc Natl Acad Sci USA. 2012; 109:E2561–2568. [PubMed: 22908292]

Young KD. The selective value of bacterial shape. Microbiol Mol Biol Rev. 2006; 70:660–703. [PubMed: 16959965]

Young KD. Bacterial shape: two-dimensional questions and possibilities. Annu Rev Microbiol. 2010; 64:223–240. [PubMed: 20825347]

Yuasa R, Levinthal M, Nikaido H. Biosynthesis of cell wall lipopolysaccharide in mutants of *Salmonella*. V. A mutant of *Salmonella typhimurium* defective in the synthesis of cytidine diphosphoabequose. J Bacteriol. 1969; 100:433–444. [PubMed: 4899003]

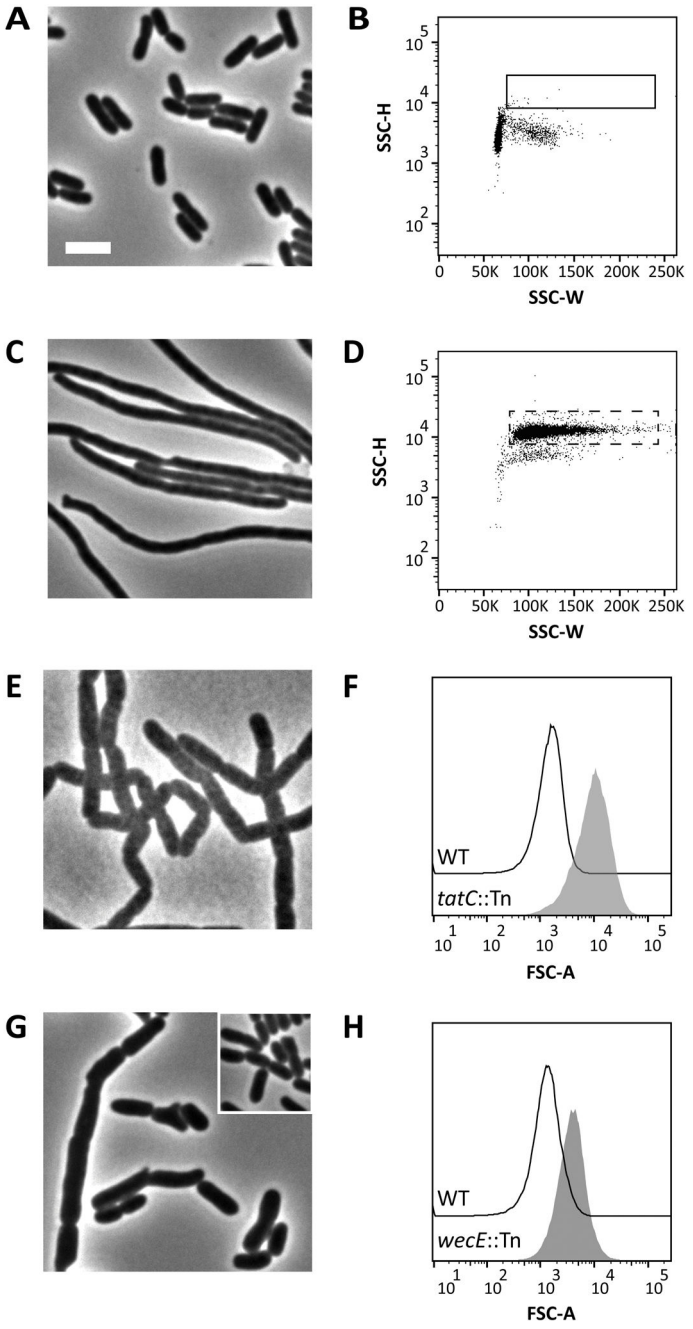

Figure 1. A genetic screen for shape mutants

(A) Phase-contrast micrograph of *E. coli* CS109 wild-type (WT) cells. The white bar represents 4 μm. (B) Flow cytometry of the WT population displayed as a dot plot with side scatter height (SSC-H) plotted against side scatter width (SSC-W). The box denotes the gate (approximately 0.1% of the population) used to sort cells from a transposon library constructed in CS109. The transposon library population looked similar to the WT when analyzed by flow cytometry. (C) Phase-contrast micrograph of WT cells treated with aztreonam (2 μg ml^{-1}) for 40 minutes. (D) Flow cytometry of aztreonam-treated cells. The

dashed box represents the same population outlined in panel B. (E) Phase-contrast micrograph of a *tatC* insertion mutant identified by the shape screen. (F) Histograms of forward scatter area for cells from the Δ*tatC*::Tn mutant (grey-filled peak) and the WT (black line). Mean of the forward scatter area as reported in arbitrary units (AU): WT=1668 AU; Δ*tatC*::Tn=11,493 AU. (G) Phase-contrast micrograph of a *wecE* insertion mutant identified by the shape screen. WT cells (inset) are shown for comparison. (H) Histograms of forward scatter area for cells from the Δ*wecE*::Tn mutant (grey-filled peak) and the WT (black line). Mean of the forward scatter area: WT=1504 AU; Δ*wecE*::Tn=4423 AU. All flow cytometry data is from 100,000 events (cells). Strains: MAJ3 (WT), MAJ165 (Δ*wecE*::Tn), and MAJ166 (Δ*tatC*::Tn).

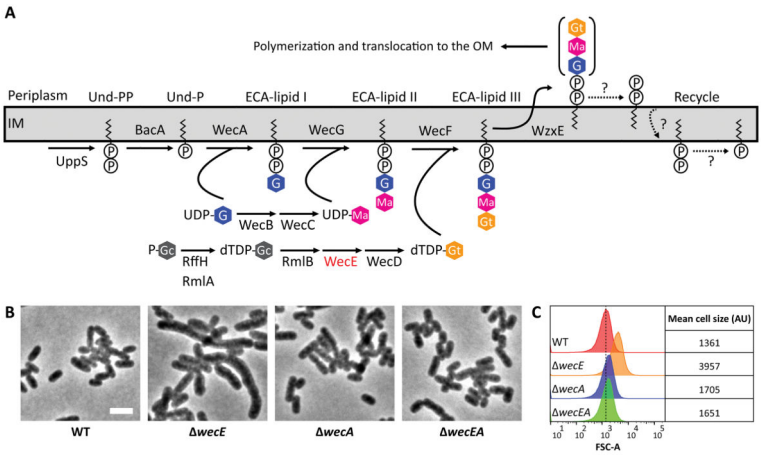

Figure 2. ECA is not required to maintain cell shape in *E. coli*

(A) ECA biosynthesis pathway. Abbreviations: P-Gc, Glucose 1-phosphate; UDP, uridine diphosphate; G, *N*-acetylglucosamine; dTDP, thymidine diphosphate; Ma, *N*-acetyl-D-mannosaminuronic acid; Gt, 4-acetamido-4,6-dideoxy-D-galactose. In *E. coli*, loss of RffH is compensated for by RmlA. RmlA is involved in the synthesis of dTDP-L-rhamnose, an O-antigen precursor (Stevenson *et al.*, 1994). The figure was adapted from Paradis-Bleau *et al.* (Paradis-Bleau *et al.*, 2014). (B) Phenotypes of Δ*wecE* mutant cells. Cells were grown at 37°C in LB to an OD_{600}=0.5–0.6, then fixed and photographed by phase-contrast microscopy. The white bar represents 4 μm. (C) Flow cytometry. Histograms of the FSC-A of live cells shown in panel B. The dashed line represents the mean forward scatter area of the WT. Mean of the forward scatter area is reported in arbitrary units (AU). Flow cytometry data is from 100,000 events (cells). Data is representative of two independent experiments. Strains: MAJ3 (WT), MAJ73 (Δ*wecE*), MAJ89 (Δ*wecA*), and MAJ90 (Δ*wecEA*).

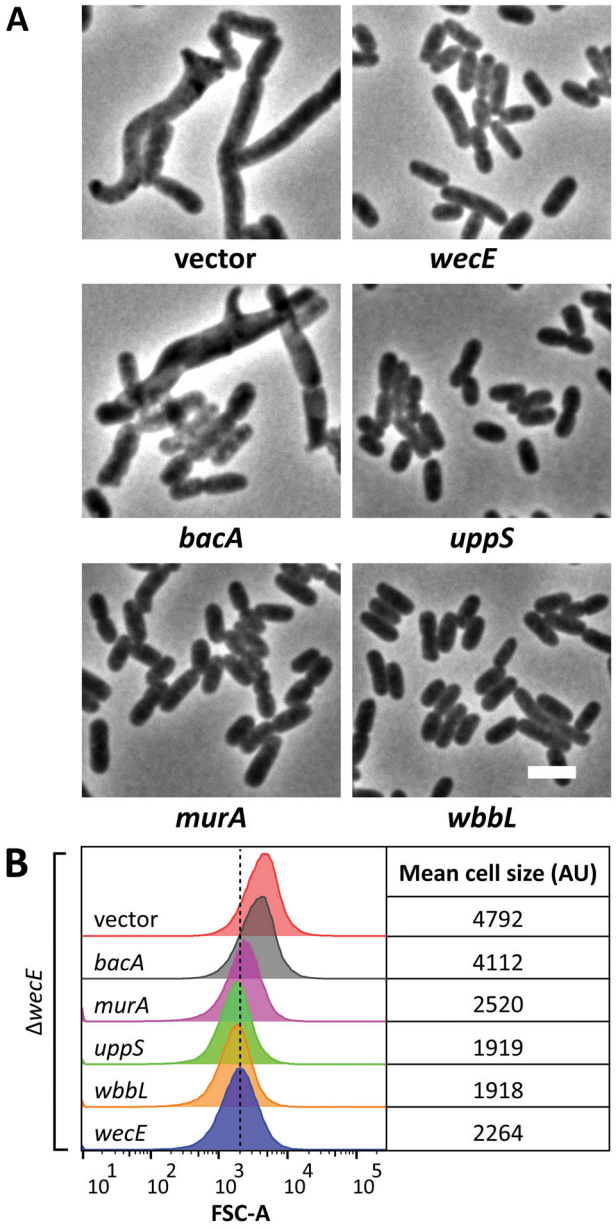

Figure 3. Suppression of Δ*wecE* shape defects

(A) Shape. Δ*wecE* cells harboring plasmids carrying the indicated genes were grown to an OD_{600} = 0.5–0.6 at 37°C in LB containing 25 μM IPTG. Cells were fixed, then photographed by phase-contrast microscopy. The white bar represents 4 μm. (B) Flow cytometry. Histograms of the forward scatter area of live cells shown in panel A. The vertical dashed line represents the mean forward scatter area of the Δ*wecE* mutant containing a plasmid expressing *wecE* (blue graph). Mean of the forward scatter area is reported in arbitrary units (AU). Flow cytometry data is from 100,000 events (cells). Data is representative of two independent experiments. Strains: MAJ78 (vector), MAJ79 (*wecE*), MAJ92 (*uppS*), MAJ135 (*bacA*), MAJ181 (*uppS*), and MAJ238 (*wbbL*).

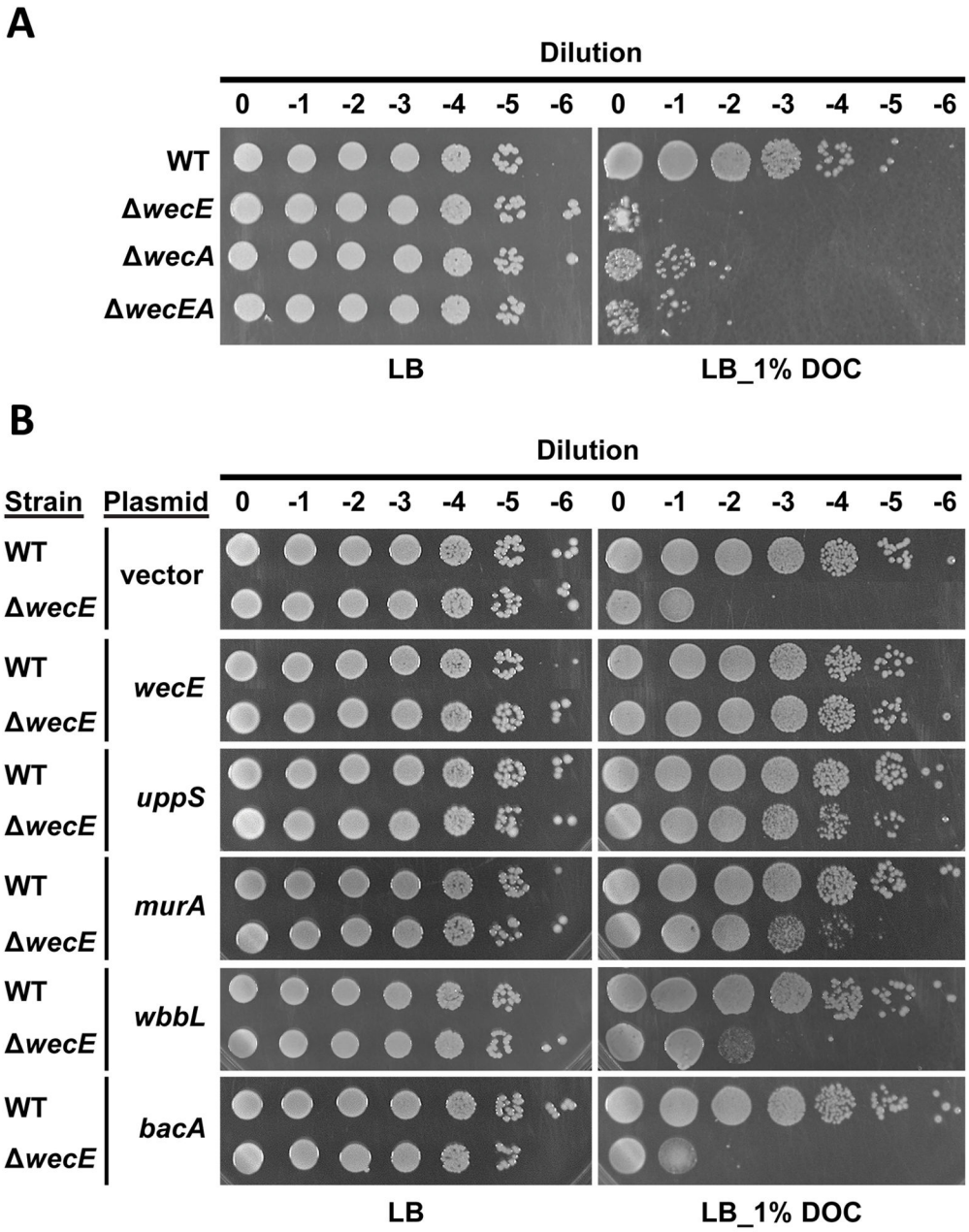

Figure 4. Suppression of Δ*wecE* bile salt sensitivity

Overnight cultures were normalized to an OD_{600} ~1.0, and 10-fold serial dilutions were plated onto LB or LB containing 1% deoxycholate. Strains shown are listed in the legend to Fig. 2 (panel A) and Fig. 3 (panel B). IPTG was not included in the plates shown in panel B. Data is representative of two independent experiments.

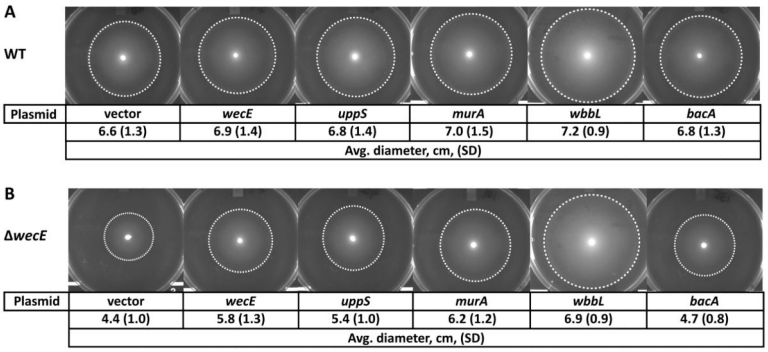

Plasmid	vector	*wecE*	*uppS*	*murA*	*wbbL*	*bacA*
	6.6 (1.3)	6.9 (1.4)	6.8 (1.4)	7.0 (1.5)	7.2 (0.9)	6.8 (1.3)
	Avg. diameter, cm, (SD)					

Plasmid	vector	*wecE*	*uppS*	*murA*	*wbbL*	*bacA*
	4.4 (1.0)	5.8 (1.3)	5.4 (1.0)	6.2 (1.2)	6.9 (0.9)	4.7 (0.8)
	Avg. diameter, cm, (SD)					

Figure 5. Suppression of Δ*wecE* motility defects

(A–B) Migration assays. Overnight cultures were spotted onto migration agar, incubated for 18 h at 30°C and then photographed. The dashed circles outline the outer extent of cell migration. Diameter data is from three independent experiments. Strains in panel A: MAJ76 (vector), MAJ77 (*wecE*), MAJ91 (*uppS*), MAJ134 (*bacA*), MAJ180 (*murA*), and MAJ237 (*wbbL*). Strain names in panel B are listed in the legend to Fig. 3

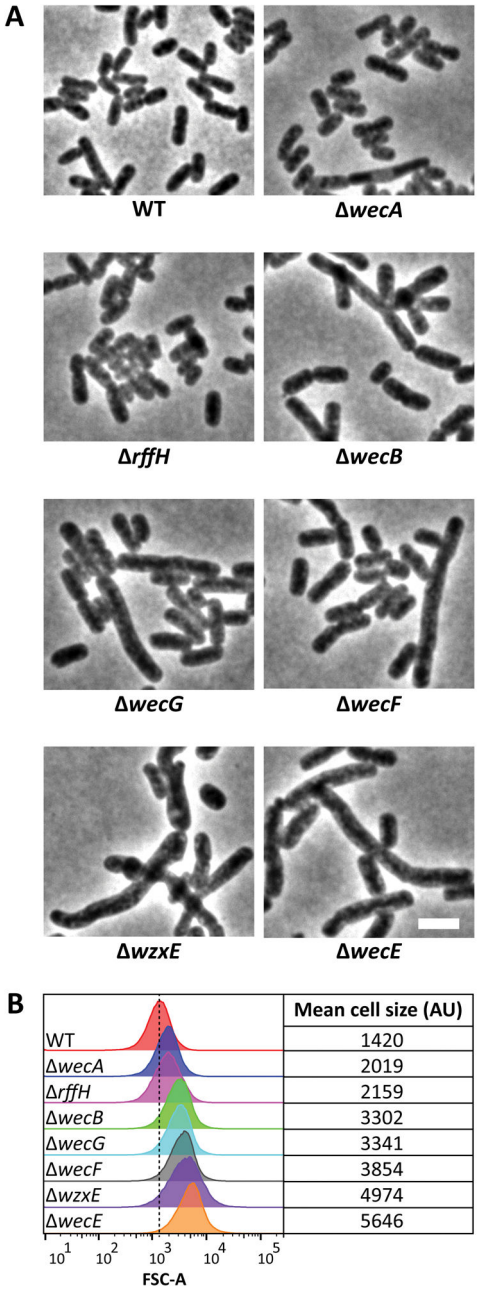

Figure 6. Shape defects of ECA mutants

(A) Shape. Cells with the indicated genotypes were grown in LB at 37°C to an OD_{600}=0.5–0.6, fixed, and photographed by phase contrast microscopy. (B) Flow cytometry. Histograms of the forward scatter area of live cells shown in panel A. The vertical dashed line represents the mean forward scatter area of the WT. Mean of the forward scatter area is reported in arbitrary units (AU). Flow cytometry data is from 100,000 events (cells). Strains: MAJ3 (WT), MAJ73 (Δ*wecE*), MAJ101 (Δ*wecA*), MAJ102 (Δ*wecB*), MAJ103 (Δ*wecF*), MAJ104 (Δ*wzxE*), MAJ118 (Δ*rffH*), and MAJ119 (Δ*wecG*).

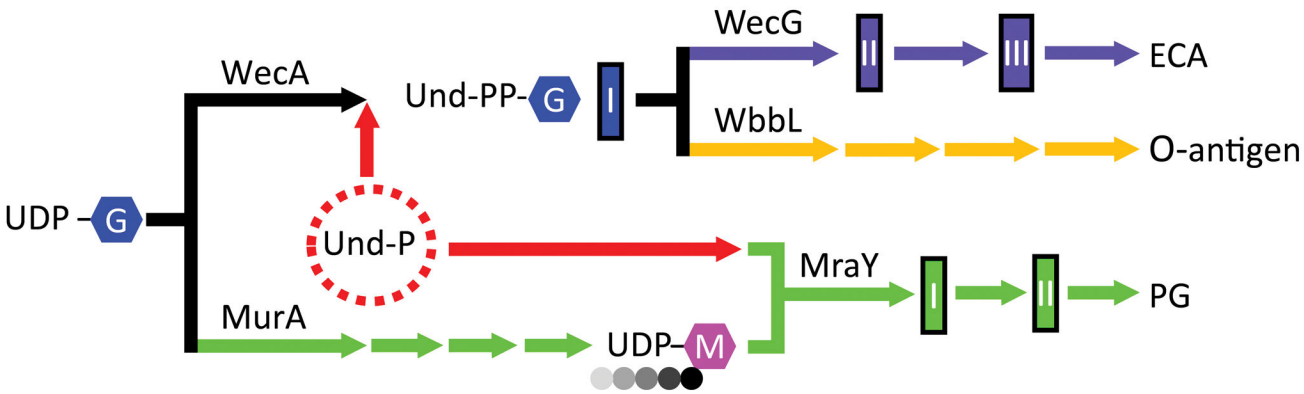

Figure 7. Model of substrate competition among metabolic pathways

The enterobacterial common antigen (ECA), O-antigen, and peptidoglycan (PG) biosynthesis pathways compete for a pool of uridine diphosphate *N*-acetylglucosamine (UDP-G) and undecaprenyl phosphate (Und-P). *E. coli* K-12 strains do not normally produce O-antigen because of an insertion in *wbbL*. Short peptides (circles) are attached to the *N*-acetylmuramic acid (M) residue. ECA-lipid I is noted in blue. ECA-lipid II and III are noted in purple. PG-lipid I and II are noted in green. Note that the colanic acid synthesis pathway also utilizes Und-P, but this pathway is omitted from the schematic. Other abbreviations: Und-PP-G, undecaprenyl pyrophosphate *N*-acetylglucosamine.

Table 1

Morphological phenotypes of an *E. coli wecE* mutant

Genotype[a]	Temp (°C)	No. of cells evaluated	Avg. length, μm, (SD)	Avg. width, μm (SD)	% cells with indicated no. of constrictions		
					0	1	>1
WT	25	323	4.4 (1.2)	1.1 (0.1)	76	24	0
	30	335	4.5 (1.1)	1.1 (0.1)	72	28	0
	37	284	4.3 (1.0)	1.2 (0.1)	68	32	0
Δ*wecE*	25	308	5.8 (4.0)	1.2 (0.1)	73	27	0
	30	281	6.9 (4.5)	1.3 (0.1)	66	33	1
	37	315	7.5 (5.2)	1.5 (0.2)	71	28	1

[a]Strains: MAJ3 (WT) and MAJ73 (Δ*wecE*).